ORNL/TM-2001/27

Field Research Center
Oak Ridge, Tennessee

Waste Characteristics of the Former S-3 Ponds and Outline of Uranium Chemistry Relevant to NABIR Field Research Center Studies

MARCH 2001

Prepared by
Scott C. Brooks
Environmental Sciences Division

ORNL/TM-2001/27

WASTE CHARACTERISTICS OF THE FORMER S-3 PONDS AND OUTLINE OF URANIUM CHEMISTRY RELEVANT TO NABIR FIELD RESEARCH CENTER STUDIES

Scott C. Brooks

March 2001

Prepared by
OAK RIDGE NATIONAL LABORATORY
P.O. Box 2008
Oak Ridge, Tennessee 37831-6285
managed by
UT-Battelle, LLC
for the
U.S. DEPARTMENT OF ENERGY
under contract DE-AC05-00OR22725

CONTENTS

LIST OF FIGURES

Figure **Page**

LIST OF TABLES

Table **Page**

ACRONYMS

DOE	Department of Energy
FRC	Field Research Center
IAP	ion activity product
NABIR	Natural and Accelerated Bioremediation
ORNL	Oak Ridge National Laboratory
PI	principal investigator
SCM	surface complexation modeling
SI	saturation index
U	uranium

1. INTRODUCTION

The Environmental Sciences Division at Oak Ridge National Laboratory (ORNL) was awarded the first Naturaland Accelerated Bioremediation Research (NABIR) Program, Field Research Cent& (FRC) based upon the recommendation of a review panel following a competitive peer-reviewed proposal process. The contaminated FRC site at ORNL is centered on groundwater plumes that originate from the former S-3 Waste Disposal Ponds located at the Y- 12 Plant and the Y- 12 Bone Yard/ Bum Yard. Proposals for individual science research projects at the FRC were submitted in the spring of 2000 in response to a solicitation issued by the Department of Energy (DOE). Proposals selected for funding began work in Fiscal Year 2001 (October 1, 2000). The FRC staff have initiated several characterization efforts intended to support, inform, and educate individual FRC investigators, NABIR principal investigators (PIs), and the broader community of the specific conditions, opportunities, and challenges of this site. These efforts include both physical site characterization as well as numerical simulation (modeling) studies.

Geochemicalmodeling has been conducted with the goal of: (1) providing a baseline understanding of the geochemical behavior of uranium (U); (2) examining the interaction of geochemistry and uranium transport in the subsurface; (3) elucidating some potential pitfalls for researchers with respect to manipulating subsurface environments for the purpose of demonstrating bacterially induced U immobilization. The geochemical modeling effort focused on using existing data and resources and did not involve the collection of new data or samples from the field site. Specifically, the following three tasks have been performed to date. (1) Searching for information on the wastes disposed in to the S-3 ponds. These data are typically found in internal technical reports at the labs and are rarely published in the peer-reviewed literature; thus, this information can be very difficult for the scientific community to access. Therefore, these searches may provide a nontrivial resource to investigators. To that end, some analytical data have already been located and the search for more data will continue. (2) Critical evaluation of thermodynamic data that are needed in the modeling calculations. (3) Generating model simulations to illustrate important aspects of U geochemistry and transport behavior in idealized solutions. This report summarizes the results of the geochemical modeling efforts .

2. HISTORICAL SKETCH OF THE S-3 DISPOSAL PONDS

In 1951, four unlined impoundments covering a total of about 1.44 ha were constructed at the western margin of the Oak Ridge Y-12 Plant in Bear Creek Valley. The impoundments were known as the S-3 ponds and each had a storage capacity of about 9.5 million liters. The ponds are no longer operational and have been covered with a multilayered Resource Conservation and Recovery Act cap and asphalt surface. The site now serves as a parking lot.

Over their 32 year operational lifetime, the S-3 ponds received liquid wastes generated from uranium operations at the Y-12 Plant, primarily acidic uranium nitrate (30% uranium nitrate), although contributions from other processes (e.g., acid washing of metals; mop water) and liquid wastes and sludges from other sites (e.g., East Tennessee Technology Park and X-10 sites in Oak Ridge, Savannah River site, Idaho National Engineering Lab) added a variety of other components to the waste stream (Al, F, K, SO_4^{2-}, ^{99}Tc, ^{239}Pu) (Tables 2.1 and 2.2). The composition of the sludges and liquids in the ponds varied from pond to pond and temporally. Nevertheless, the liquid waste in the ponds can generally be described as highly acidic (primarily nitric acid) and the major metallic constituents were calcium (Ca), magnesium (Mg), sodium (Na), potassium (K), and aluminum (Al), with moderately high concentrations of trace metals. In 1976, a nitrate recovery and recycle system reduced nitrate discharges to the impoundments but there was no change in the amount of uranium discharged (Table 2.3).

In 1983 waste discharges to the ponds ceased and the wastes remaining in the ponds were treated in *situ* by neutralization and biodenitrification. After this treatment, the sludges were allowed to settle and the supematant liquid pumped off and treated for removal of organic contaminants and metals. The treated water was subsequently discharged to the East Fork Poplar Creek. Prior to tilling and capping the S-3 ponds, contaminated sludges from the "Blue Lagoons" area west of the S-3 ponds were added to the southwest pond.

Table 2.1. Chemical analyses of the iiquid wastes collected from the S-3 disposal ponds, 1978 (all values are in mg/L, except pH.; reproduced from Jeter and Napier, 1978). Only inorganic constituents of the waste are shown.*

	Northeast Pond		Northwest Pond		Southwest Pond		Southeast Pond †	
	Top	Bottom	Top	Bottom	Top	Bottom	Top	Bottom
pH	1.2	0.8	1.1	0.8	1.4	1.2	4.2	5.3
Cl^-	2,330	1,641	1,600	1,003	687	789	207	286
F^-	9	25	8	31	5	4	9	1
NO_3^-	17,840	73,840	21,560	69,100	11,020	20,460	7,590	10,410
U ‡	139.57	316.57	180.81	313.	80.34	111.21	17.51	3.24
Ag	0.6	1.8	0.5	1.8	0.2	0.4	<0.1	<0.1
Al	1,202	4,522	1,346	4,858	668	1,370	300	8.5
As	0.028	0.115	0.028	0.07	0.013	0.025	0.001	0.003
B	30	17	21	8.1	8.5	7.1	2.6	1.6

Table 2.1. (continued)

	Northeast Pond		Northwest Pond		Southwest Pond		Southeast Pond †	
	Top	Bottom	Top	Bottom	Top	Bottom	Top	Bottom
Ba	0.4	0.7	0.5	4.4	0.3	0.7	0.8	0.5
Ca	267	877	276	840	137	250	1,381	3,053
Cd	0.7	158	08	5.4	0.4	2.0	0.3	0.7
co	0.5	1.1	0.5	1.4	0.4	0.5	0.2	0.4
Cr	60	37	43	34	11.9	11.6	8.5	<0.1
Cu	13.2	44	12.8	32	6.0	10.5	3.9	0.3
Fe	168	765	174	1208	88	347	0.8	1.8
Hg	0.052	0.320	0.062	0.24	0.032	0.064	0.004	0.003
K	90	310	86	416	43	109	93	98
Li	12	32	9.5	25	4.1	7.9	5.1	6.9
Mg	169	654	198	672	99	199	125	190
Mn	7.5	24	9.1	22	5.2	11	8.3	12
Na	3.475	2,300	2,617	1,128	1,234	1,262	652	664
Ni	55	128	47	50	22	31	16	39
P	59	101	49	70	21	27	1.0	<0.1
Se	0.018	0.003	0.033		0.029	0.022	0.005	0.002
Si	32	70	33	94	<1	51	<1.0	<1.0
Sr	1.0	3.7	1.2	4.9	0.6	1.2	1.2	1.1
Th	20	85	26	118	1.28		0.2	0.1
Ti	2.0	6.4	2.2	70	1.0	1.4	<0.1	<0.1
Y	<0.1	0.3	0.1	0.2	<0.1	<0.1	<0.1	<0.1
Zn	8.5	12	5.6	10	2.2	4.0	1.9	1.4
Zr	2.0	8.0	2.5	11	1.2	2.7	<0.1	<0.1

* Waste discharges into the S-3 ponds entered in the Northeast cell and proceeded sequentially via overflow conduits to the Northwest, Southwest, and Southeast cells. Apparently, samples were not analyzed for sulfate; later characterization of the sludges indicated sulfate concentrations of about 2000 mg/kg.

† After 1975, the Southeast cell was used to dispose of biodenitrification sludge and alkaline waste ($CaCO_3$ and KOH). Between 1975 and 1978, the pH in this pond increased from 0.8 to 4.8.

‡ 99.67% ^{238}U

Table 2.2. Chemical analyses of sludges from the S-3 disposal ponds, 1983 (all values are in µg/gram dry weight; reproduced from report Y/MA-6400, 1983). Only inorganic constituents are shown.*

	Northeast Pond	Northwest Pond	Southwest Pond	Southeast Pond †
Ag	17.0	4.1	2.1	7.3
Al	41,854.0	24,643.8	59,034.9	41,897.8
As	32.5	21.7	26.0	14.8
B	98.7	55.7	138.6	70.0
Ba	428.6	337.3	285.9	359.4
Be	1.3	1.4	2.9	16.4
Ca	1,005.5	894.3	1,952.2	3,962.9
Cd	<0.6	<0.6	<0.6	<0.6
Ce	45.9	72.3	73.3	48.0
Co	1.6	<0.01	1.4	3.3
Cr	75.9	48.5	135.1	163.9
Cu	136.4	128.2	111.1	145.3
Fe	89,500.0	8,232.8	26,284.2	92,031.0
Ga	1.6	30.5	33.5	11.9
Hf	4.9	14.0	14.3	19.4
Hg	1.7	0.21	0.88	12.0
K	11,070.6	8,307.9	23,762.6	8,000.3
La	37.7	45.7	42.1	25.5
Li	46.9	29.2	35.1	46.3
Mg	2,614.7	1,593.7	4,437.0	2,341.1
Mn	108.1	45.9	63.1	112.0
Mo	103.8	30.1	113.7	191.7
Na	1,768.9	2,041.0	1,993.5	1,429.5
Nb	62.0	45.6	30.9	136.8
Ni	73.9	62.9	60.6	98.8
P	1,333.5	2,296.9	2,454.8	6,896.4
Pb	198.1	207.0	155.0	119.7

Table 2.2 (continued)

	Northeast Pond	Northwest Pond	Southwest Pond	Southeast Pond †
Sc	8.1	4.6	8.4	5.6
Se	<0.2	<0.2	<0.2	<0.2
Si	37.5	22.7	666.0	40.9
Sr	46.0	66.5	62.3	40.3
Th	150.0	529.4	196.0	271.7
Ti	5,172.1	5,206.1	5,120.1	3,630.5
U ‡	280.0	300.0	410.0	620.0
V	61.5	26.5	64.7	63.1
Y	12.5	11.6	12.1	8.4
Zn	95.0	34.0	56.3	91.2
Zr	817.7	3.366.0	1,077.4	1,472.0

* Waste discharges into the S-3 ponds entered in the Northeast cell and proceeded sequentially via overflow conduits to the Northwest, Southwest, and Southeast cells. Apparently, samples were not analyzed for sulfate; later characterization of the sludges indicated sulfate concentrations of about 2,000 mg/kg.

† After 1975, the Southeast cell was used to dispose of biodenitrification sludge and alkaline waste ($CaCO_3$ and KOH). Between 1975 and 1978, the pH in this pond increased from 0.8 to 4.8.

‡ 99.5% ^{238}U

Table 2.3. Total nitrate content of the S-3 disposal ponds by year*

Year	Nitrate Content (kg)
1962	2263000
1975	1866000
1978	993000
1981	581000
1983	978000

***Reproduced from report Y/MA-6400, 1983.**

3. BASICS OF AQUEOUS CHEMISTRY OF URANIUM

Uranium contamination of soils and groundwater surrounding the S-3 ponds is one of the drivers demanding remedial action at the FRC site. Areas near the ponds were contaminated due to the nature of both the ponds (seepage ponds) and the wastes. The appearance of uranium farther away from the ponds results from interaction of the intruding waste with resident fluids, soil and aquifer minerals, and solute transport. The geochemistry of uranium and the reactions of the waste with soil and aquifer minerals, coupled with the site hydrology, can be used to understand what factors contribute to the movement of this solute in groundwater at the FRC site. Part of the reason uranium has moved down the valley lies in the physical hydrology of the system (rapid flow through conductive fracture networlc). In this report we examine several chemical processes that influence uranium transport: hydrolysis, complexation equilibria, and sorption. Sorption serves as a mechanism to reduce uranium mobility (ignoring sorption to mobile colloids for the sake of simplicity). Hydrolysis and aqueous complexation change the charge and composition of uranium in solution and may increase uranium solubility, decreasing the effectiveness of sorptive mechanisms in slowing the movement of uranium.,

Another mechanism that can remove U from solution and slow its movement in groundwater is precipitation. Recent work has suggested that at U concentrations ~ 10^{-9} M the time scale for uranium precipitation in groundwater systems is on the order of centuries (Luo et al., 2000). The relative importance of non-microbial uranium precipitation at the FRC site (U concentrations ~ 10^{-5} M) is difficult to assess without direct examination of solid phase materials. Nevertheless, most of the water analyses that were examined for this report indicated that the waters were undersaturated with respect to most uranium minerals. This observation, in conjunction with the slow kinetics of precipitation suggests that this process does not exert a major control on U solubility at the FRC site. For the purposes of this report, precipitation of U minerals was not allowed although the degree of saturation with respect to the solid phases β-$UO_2(OH)_2$ and UO_2CO_3 was considered.

Some documents related to site characterization speculate that U discharged to the S-3 ponds was in some combination of the IV, V, and VI oxidation states. However, neither the wastes nor the pond fluids or sludges were analyzed to determine U oxidation state. Given the low solubility of U(IV) and the rapid oxidation kinetics of U(IV) and U(V), we assume that all the U is in the hexavalent state (U(VI)).

Uranium hydrolysis, aqueous complexation, precipitation, and sorption are explored below. These processes are illustrated by geochemical modeling using a fluid with 10^{-5} M UO_2^{2+} and ionic strength (I) = 0.2. These values were chosen as an approximation to the water analysis data from wells in the vicinity of the S-3 ponds at the FRC site. Modeling results presented in this report may differ in specifics from other published reports that have used different modeling assumptions (e.g., different ionic strength or U_{TOT}); nevertheless, the general aspects of the modeling results are similar. Thermodynamic constants used in the modeling are given in Table 3.1 below. The thermodynamic data were used for the aqueous speciation and sorption modeling in this report. The subscript "s" for the surface complexation reactions designates strong sites, whereas the subscript "w" designates weak sites. Where no distinction among sites is made, the log K value is assumed to be the same for both strong and weak sites.

Table 3.1 Thermodynamic constants used in geochemical modeling.

	Metal Hydrolysis	log K (25°C, $I = 0$)	Source
1	$UO_2^{2+} + H_2O = UO_2OH^+ + H+$	-5.2	a
2	$UO_2^{2+} + 2\,H_2O = UO_2(OH)_{2(aq)} + 2H^+$	-10.3	a
3	$UO_2^{2+} - 3H_2O = UO_2(OH)_3^- + 3H^+$	-19.2	a
4	$UO_2^{2+} + 4H_2O = UO_2(OH)_4^{2-} + 4H^+$	-33.0	a
5	$2UO_2^{2+} - H_2O = (UO_2)_2OH^{3+} + H^+$	-2.7	a
6	$2UO_2^{2+} - 2H_2O = (UO_2)_2(OH)_2^{2+} + 2H^+$	-5.62	a
7	$3UO_2^{2+} + 4H_2O = (UO_2)_3(OH)_4^{2+} + 4H^+$	-11.9	a
8	$3UO_2^{2+} - 5H_2O = (UO_2)_3(OH)_5^+ + 5H^+$	-15.5	a
9	$2UO_2^{2+} + 7H_2O = (UO_2)_3(OH)_7^- + 7H^+$	-31.0	a
Carbonate Complexes			
10	$UO_2^{2+} + CO_3^{2-} = UO_2CO_{3(aq)}$	9.68	a
11	$uo_2^{2+} + 2CO_3^{2-} = UO_2(CO_3)_2^{2-}$	16.94	a
12	$UO_2^{2+} + 3CO_3^{2-} = UO_2(CO_3)_3^{4-}$	21.6	a
13	$3UO_2^{2+} + 6CO_3^{2-} = (UO_2)_3(CO_3)_6^{6-}$	54.0	a
14	$2UO_2^{2+} + 4H_2O + CO_{2(g)} = (UO_2)_2CO_3(OH)_3^- + 5H^+$	-19.01	a
Solid Phases			
15	$\beta\text{-}UO_2(OH)_{2(s)} + 2H^+ = UO_2^{2+} + 2H_2O$	4.93	a*
16	$UO_2CO_3 = UO_2^{2+} + CO_3^{2-}$	-14.47	a
Surface Protonation Reactions			
17	$>FeOH + H^+ = >FeOH_2^+$	6.5 1	b
18	$>FeOH = FeO^- + H^+$	-9.13	b
Surface Complexation Reactions			
19	$(>Fe_s(OH)_2) + UO_2^{2+} = (>Fe_sO_2)UO_2 + 2H^+$	-2.57	b
20	$(>Fe_w(OH)_2) + UO_2^{2+} = (>Fe_wO_2)UO_2 + 2H^+$	-6.28	b
21	$>FeOH + H_2CO_3 = >FeCO_3H + H_2O$	2.90	b
22	$>FeOH + H_2CO_3 = >FeCO_3^- + H_2O + H^+$	-5.09	b
23	$(>Fe_s(OH)_2) + UO_2^{2+} + CO_3^{2-} = (>Fe_sO_2)UO_2CO_3^{2-} + 2H^+$	3.67	b
24	$(>Fe_w(OH)_2) + UO_2^{2+} + CO_3^{2-} = (>Fe_wO_2)UO_2CO_3^{2-} + 2H^+$	-0.42	b

*derived from ΔG_f° values reported by Grenthe et al. (1992).

[a]Grenthe ct al., 1992.

[b] Waite et al., 1994.

3.1 HYDROLYSIS REACTIONS.

Hydrolysis results in the formation of aqueous species and solid hydroxides by the action of water. Hydrolysis reactions thereby change the composition and net charge of the metal ion and exert solubility controls on water composition. These reactions are important for all the actinide elements. Uranyl hydrolysis can be represented generically as:

$$(UO_2^{2+})_m + nH_2O \rightleftharpoons (UO_2)_m(OH)_n^{2m-n} + nH^+ \qquad (1)$$

Uranyl hydrolysis begins at about pH 3 and these species become more important as the solution pH increases (Fig. 3.1) . Polymeric species ($m > 1$ in Equation (1)) become increasingly important as the total concentration of Uranium in solution increases. As indicated in Equation (1), when $n \geq 2m$ uranium exists in solution as a neutral or negatively charged species.

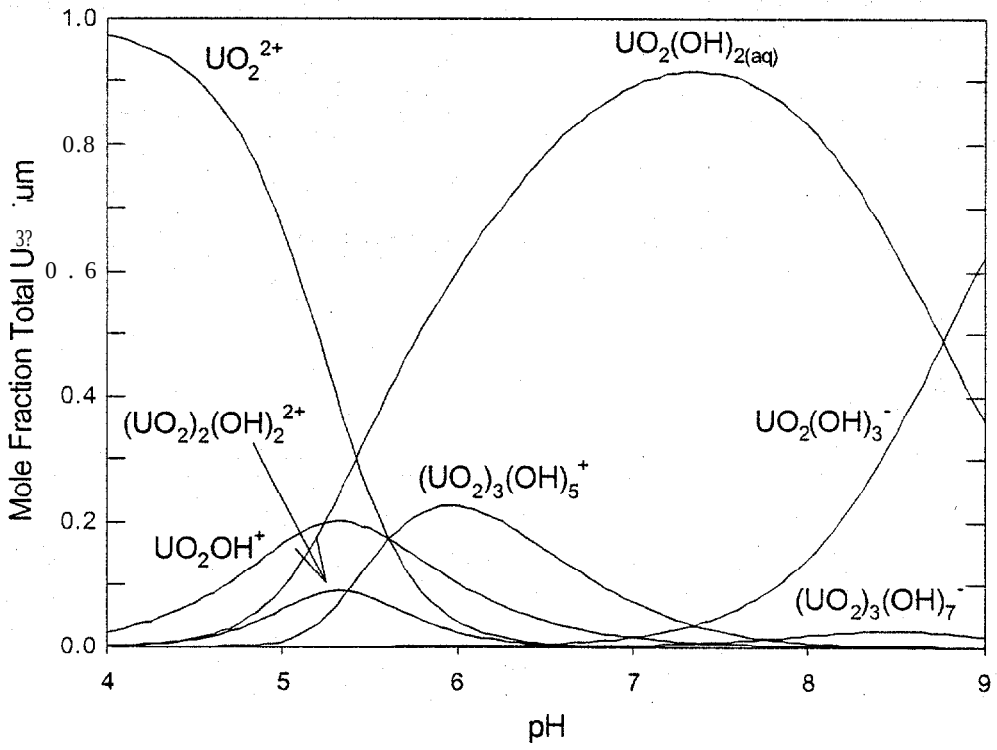

Fig. 3.1. Aqueous uranium speciation as a function of pH. Species are plotted as the mole fraction of total uranium versus solution pH. Only hydrolysis products were considered for this diagram. $U_{TOT} = 10^{-5}$ M; I = 0.2; no precipitation allowed.

3.2 COMPLEXATION EQUILIBRIA

Among the most important naturally occurring complexants for uranyl ion are the carbonate species, bicarbonate (HCO_3^-) and carbonate (CO_3^{2-}). These two species are present at significant concentrations in many natural waters and form very strong complexes with UO_2^{2+}. An understanding of this relationship led to the development of the alkali leaching process of uranium ores for the selective removal of uranium.

The S-3 ponds were excavated in saprolite which had weathered from the underlying Nolichucky shale. The Nolichucky formation has a carbonate mineral content of 11 wt% (Lee et al., 1987) and the overlying saprolite derived from it contains variable amounts of residual carbonate minerals. Part of the waste plume created from the S-3 wastes penetrated into the Nolichuclcy formation and has upwelled, mixing with shallower water and discharging into creeks down Bear Creek Valley. Thus, as the highly acidic waste percolated through the saprolite and the Nolichucky formation, there was ample opportunity for interaction with carbonate minerals to neutralize some of the acidity and for the fluid to accumulate dissolved inorganic carbon.

Aqueous speciation diagrams for uranium were generated assuming I 0^{-5} M U, I = 0.2 M and maintaining equilibrium between the solution and a gas phase with fixed partial pressure of $CO_{2(g)}$ (P_{CO2}). In different simulations, the P_{CO2} was fixed at atmospheric levels ($10^{-3.5}$) or at two different elevated P_{CO2} levels: 10^{-2} or $10^{-0.757}$. The latter value was chosen based on the analysis of water samples from the FRC site. As the concentration of total inorganic carbon exceeds the concentration of U, the carbonate species dominate U speciation (Fig. 3.2A-C). At high pH, hydrolysis products are no longer important. As the partial pressure of CO, increases, the carbonate species begin to dominate at lower pH values (cf. Fig.. 3. 2A - 2C). The results of these calculations clearly show the significant impact that carbonate complexation has on the aqueous speciation of U(VI) (Fig. 3.2A-C). The implications of these complexation reactions for uranium mobility are addressed below.

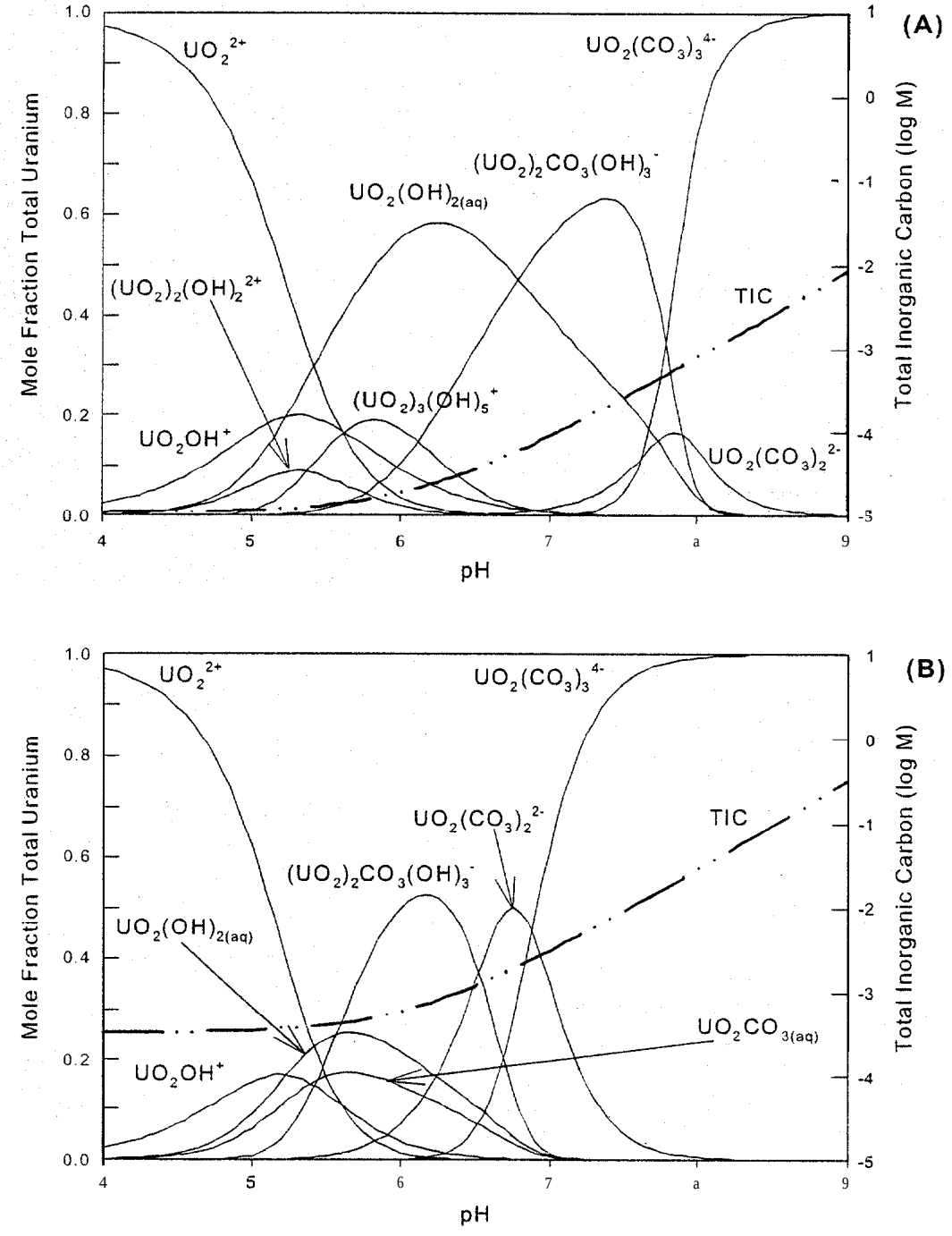

Fig.3.2. Uranium aqueous speciation as a function of pH considering both hydrolysis products and carbonate complexes. Species are plotted as mole fraction total uranium versus solution pH. $U_{TOT} = 10^{-5}$ M: I = 0.1; (A) $P_{CO2} = 10^{-3.5}$; (B) $P_{CO2} = 10^{-2.0}$; no precipitation allowed.

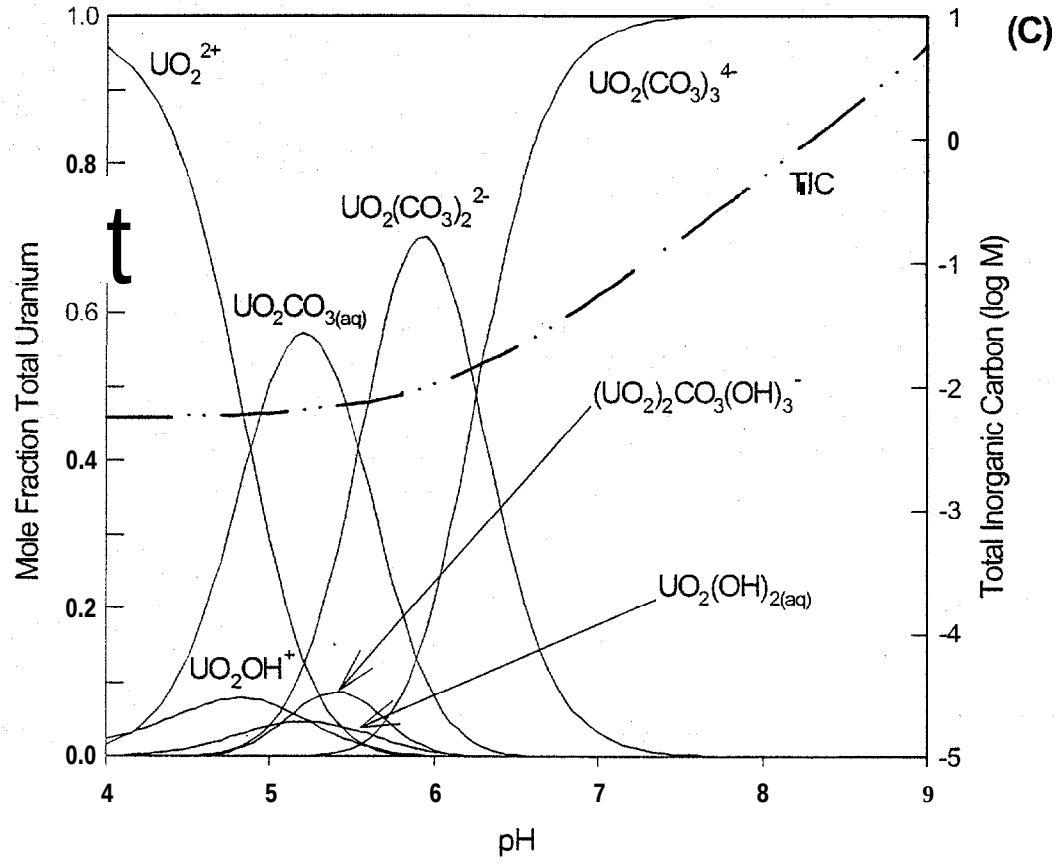

Fig. 3.2 (cont.) Uranium aqueous speciation as a function of pH considering both hydrolysis products and carbonate complexes (C). $U_{TOT} = 10^{-5}$ **M; I = 0.2; (C)** $P_{CO2} = 10^{-0.757}$; no precipitation allowed.

3.3 MINERAL SATURATION

Given a water composition, it is possible to evaluate whether the water is over- or undersaturated with respect to various mineral phases. This state is commonly expressed in terms of the saturation index (SI) which compares the product of ion activities to the equilibrium constant for the reaction. A general form for this is:

$$(A_aB_b)_{solid} \rightleftharpoons aA + bB \qquad K_{sp} = \frac{\tilde{a}_A[A]^a\ \tilde{a}_B[B]^b}{a_{A_aB_b}} \tag{2}$$

$$IAP = \tilde{a}_A[A]^a\ \tilde{a}_B[B]^b$$
$$SI = \log \frac{IAP}{K_{sp}} \tag{3}$$

in which ion activity product (IAP) is determined from the aqueous speciation of the water; [A] = concentration; γ_i = activity coefficient. An undersaturated mineralhas a negative SI (reaction (2) needs to proceed to the right to reach equilibrium), an oversaturated mineral has a positive SI (reaction (2) needs to proceed to the left to reach equilibrium), and a mineral in equilibrium with the water has an SI = 0.

The impact of hydrolysis and carbonate complexation on the aqueous speciation of U has been illustrated. For the same scenarios used above (10^{-5} M U; I = 0.2 M), we can calculate the SI with respect to β-$UO_2(OH)_2$ and UO_2CO_3 as a function of pH. In the absence of CO_2, the solution is oversaturated with respect to β-$UO_2(OH)_2$ from pH 5.8 to 8.9 (Fig. 3. 3A). Above pH 8.9, the formation of stable aqueous hydrolysis products increases the solubility of U(VI) and the SI decreases. When in equilibrium with atmospheric CO_2, the fluid is oversaturated with respect to β-$UO_2(OH)_2$ over a narrower pH range, from pH 5.8 to 7.1. At higher levels of CO_2, the solution remains undersaturated across the range of pH (Fig. 3.3A). For all levels of CO_2 examined, the solution remains undersaturated with respect UO_2CO_3 (Fig. 3.3B). The formation of stable aqueous carbonate complexes results in higher uranium solubility, making U precipitation less favorable (thus the use of alkali leaching to recover U from ore) potentially resulting in the undesirable enhanced transport of uranium.

Similar simulations were conducted for a water composition from the FRC site (well GW-83.5; http://www.esd.ornl.gov/BCV-FieldSite/). The SI with respect to β–$UO_2(OH)_2$ as a function of P_{CO2} was calculated. As the P_{CO2} comes into equilibrium with atmospheric CO_2, the water becomes over-saturated with respect to this mineral phase (Fig. 3.4). Field projects at the FRC propose to withdraw groundwater, make various amendments to promote bacterial activity in the aquifer, and reinject the water. Significant loss of CO, during these pumping operations may lead to the precipitation of U(VI) solids in the equipment or possibly the reinjection of U(VI) colloids complicating the bioreduction efforts and interpretation of results.

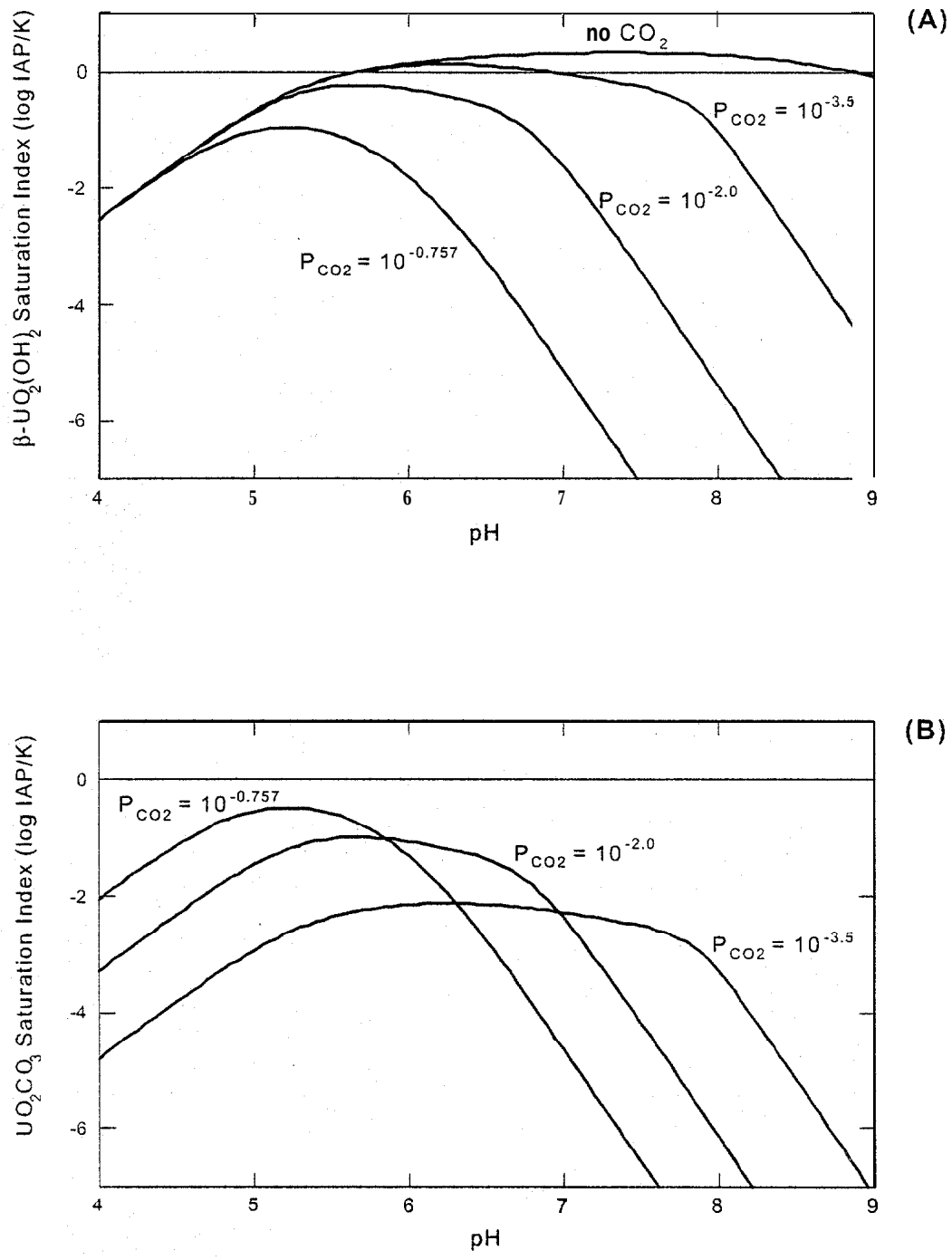

Fig. 3.3. Saturation index as a function of P_{CO2} and pH with respect to (A) β-$UO_2(OH)_2$, and (B) UO_2CO_3.

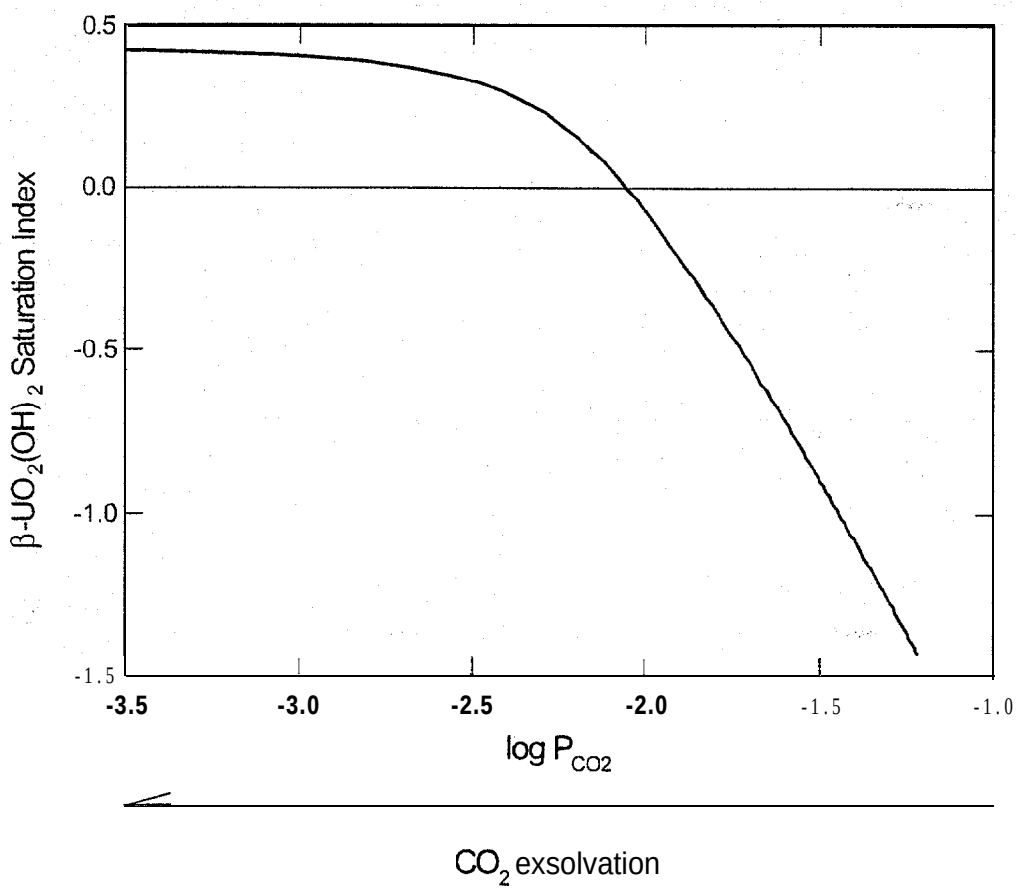

Fig. 3.4. Saturation index with respect to β-$UO_2(OH)_2$ as a function of P_{CO2} for well GW-835. Manipulations ofgroundwater that lead to loss of CO, from solution may result in the precipitation of U solids in the absence of microbial dissimilatory U reduction.

3.4 SORPTION

Sorption to aquifer solids represents another mechanism that can remove U from solution and delay its migration in the subsurface. Given the impact of hydrolysis and carbonate complexation on U(VI) speciation and saturation state, it seems likely that these processes will also play an important role in governing U sorption. To investigate these effects, a surface complexation modeling (SCM) approach was adopted using the model developed by Waite et al. (1994) (see Table 3.1). SCM explicitly accounts for changes in solution pH and ionic strength and is more generally useful than using empirical isotherms whose validity is tightly coupled to the experimental conditions under which they are measured. The model used includes aqueous U(W)-carbonate complexes and the sorption of carbonate and U(VI)-carbonate complexes. Recent X-ray Absorption Fine Structure studies support the importance of considering the latter surface species (Bargar et al., 2000).

Uranium sorption was modeled as a function of pH and P_{CO2}. In these simulations, the equilibrium pH is varied and all other conditions are held constant. The fraction of U sorbed is plotted versus pH to generate sorption edges. Modeling results are in general agreement with the experimental observations and modeling results of Waite et al. (1994) and Barnett et al. (2000). In the absence of CO_2, U(VI) displays cation-type sorption behavior - the fraction sorbed increases with increasing pH (Fig. 3.5). The fraction sorbed increases sharply over a narrow pH range and plateaus at ~ 0.95 from pH 6-8. At pH > 8, the aqueous hydrolysis products exceed the affinity of the surface for uranium and the fraction sorbed decreases. When PCO, = $10^{-3.5}$ or 10^{-2}, the initial shape of the sorption edge is similar to the no CO, case. Nevertheless, the formation of strong carbonate complexes results in a sharp decline in the fraction sorbed beginning at pH 7.5 ($P_{CO2} = 10^{-3.5}$) and pH 6 ($P_{CO2} = 10^{-2}$). At the highest P_{CO2} level examined the maximum fraction of U(VI) sorbed remains below 0.06.

Another, perhaps more familiar approach is to vary only the initialconcentration of U and hold all other conditions constant. The amount of U sorbed is plotted versus the equilibrium U concentration to generate sorption isotherms. Simulated U sorption isotherms were generated using SCM, four different CO, conditions, and pH either 5.5 or 7. These pH values were selected because they bracket the range of most of the pH measurements from wells showing U contamination at the FRC site. As expected from the sorption edges, sorption generally increases at the higher pH (Fig. 3.6). The exception occurring when the partial pressure of $CO_2 = 10^{-0.757}$. At each pH, uranium sorption decreases with increased P_{CO2}, the effect being more apparent at the higher pH. One detail shown in the isotherms is not evident from the sorption edges: the amount of uranium sorbed given an equilibrium aqueous concentration of uranium. For example, at pH 5.5 a water containing 10^{-5} M U and no carbonate species reflects a sorbed U concentration of 0.0066 mole/kg. When the P_{CO2} is 10^{-2}, the sorbed concentration would be 0.0045 mole/kg - a decrease of 32%.

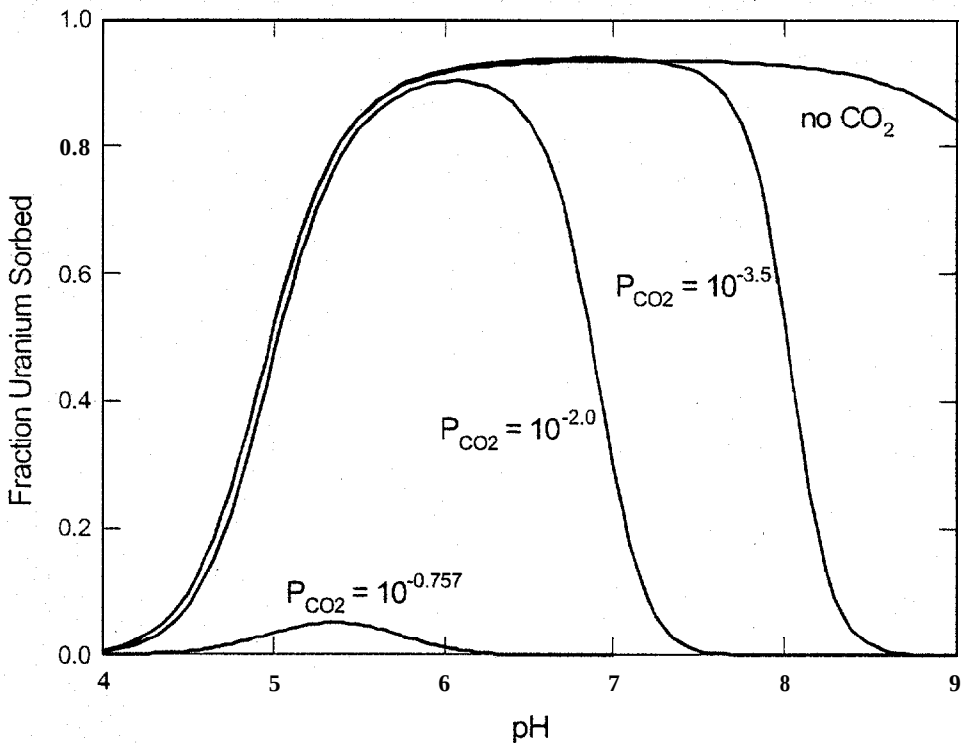

Fig. 3.5. Fraction U(VI) sorbed to solid phase as a function of pH and P_{CO2}. $U_{TOT} = 10^{-5}$ M, I = 0.2.

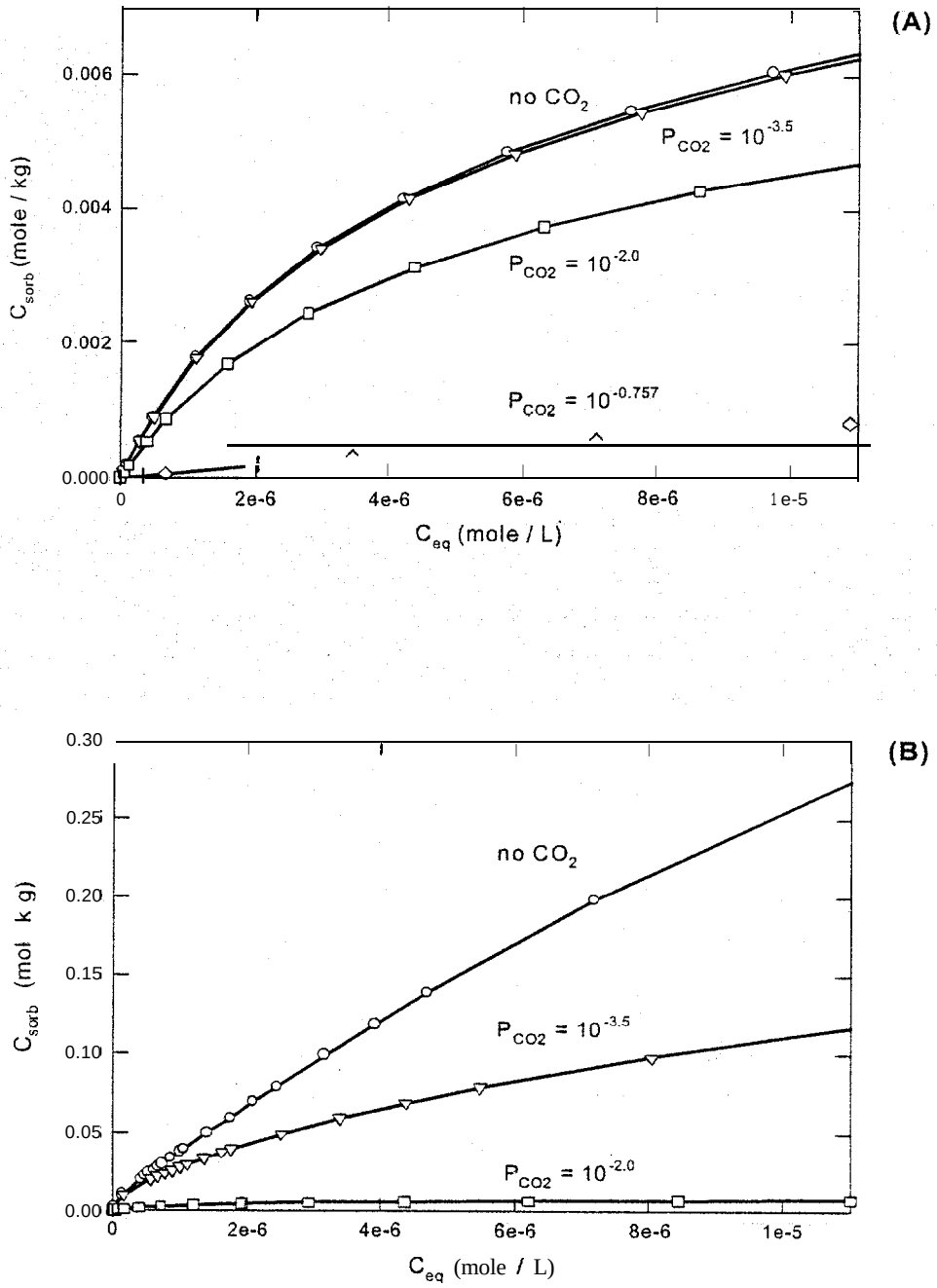

Fig. 3.6. Uranium sorption isotherms at different P_{CO2} levels using a surface complexation model approach. Ionic strength = 0.2 M, (A) pH 5.5, and (B) pH 7.0. At pH 7 and $P_{CO2} = 10^{-0.757}$ there is no U sorption.

3.5 TRANSPORT

Aqueous complexationreactions have a demonstrable effect on U(VI) solubility and sorption. To explore how these reactions might impact uranium movement in groundwater, transport simulations were run that incorporated the processes introduced above (hydrolysis, carbonate complexation, surface complexation model of adsorption). The simulations used a one-dimensional model of advective-dispersive transport assuming homogeneous, isotropic media and the pH was held constant at 7, $U_{TOT} = 10^{-5}$ M, and I = 0.2. These simulations were not meant to match observed data for U(VI) transport through saprolites (e.g., Barnett et a I., 2000) but were intended to illustrate the influence of aqueous chemistry on transport.

Results of the simulations are presented as breakthrough curves in which the relative concentration of the solute (= concentration in the sample divided by concentration in the influent solution) is plotted versus dimensionless time expressed as pore volumes. We define the uranium retardation (R) as the time at which the relative concentration of uranium reaches 50% of its influent concentration relative to that of an ideal nonreactive tracer. When no CO, is present in the system U(VI) transport shows substantial delay and R = 34 (Table 3.2, Fig. 3.7);. The delayed transport of U is a result of the accumulation of mass on the solid phase via sorption. Because sorption is modeled as a reversible equilibrium process, the mass stored on the solid phase is released when the pulse is turned off and U-free water passes through the column. U(VI) desorbs from the surface and continues to wash out for an extended time contributing to the tailing behavior seen in the breakthrough curves. As the partial pressure of CO, increases, the formation of uranyl-carbonate complexes decreases uranium retention on the solid phase and uranium transport is more rapid. When $P_{CO2} = 10^{-0.757}$ the uranium breakthrough curve is coincident with the nonreactive tracer.

A comprehensive description of the environmental chemistry of U and the actinide elements is beyond the scope of this brief study. Salient aspects that are applicable to work at the FRC have been highlighted and may serve as an entry into additional study for interested readers.

Table 3.2. Influence of P_{CO2} on U(VI) transport as indicated by U retardation factor.

Uranium Retardation (R = time when $C/C_0 = 0.5$) Relative to Nonreactive Tracer			
No co,	$P_{CO:} = 10^{-3.5}$	$P_{CO2} = 10^{-2.0}$	$P_{CO2} = 10^{-0.757}$
34.1	16.6	2.2	I.0

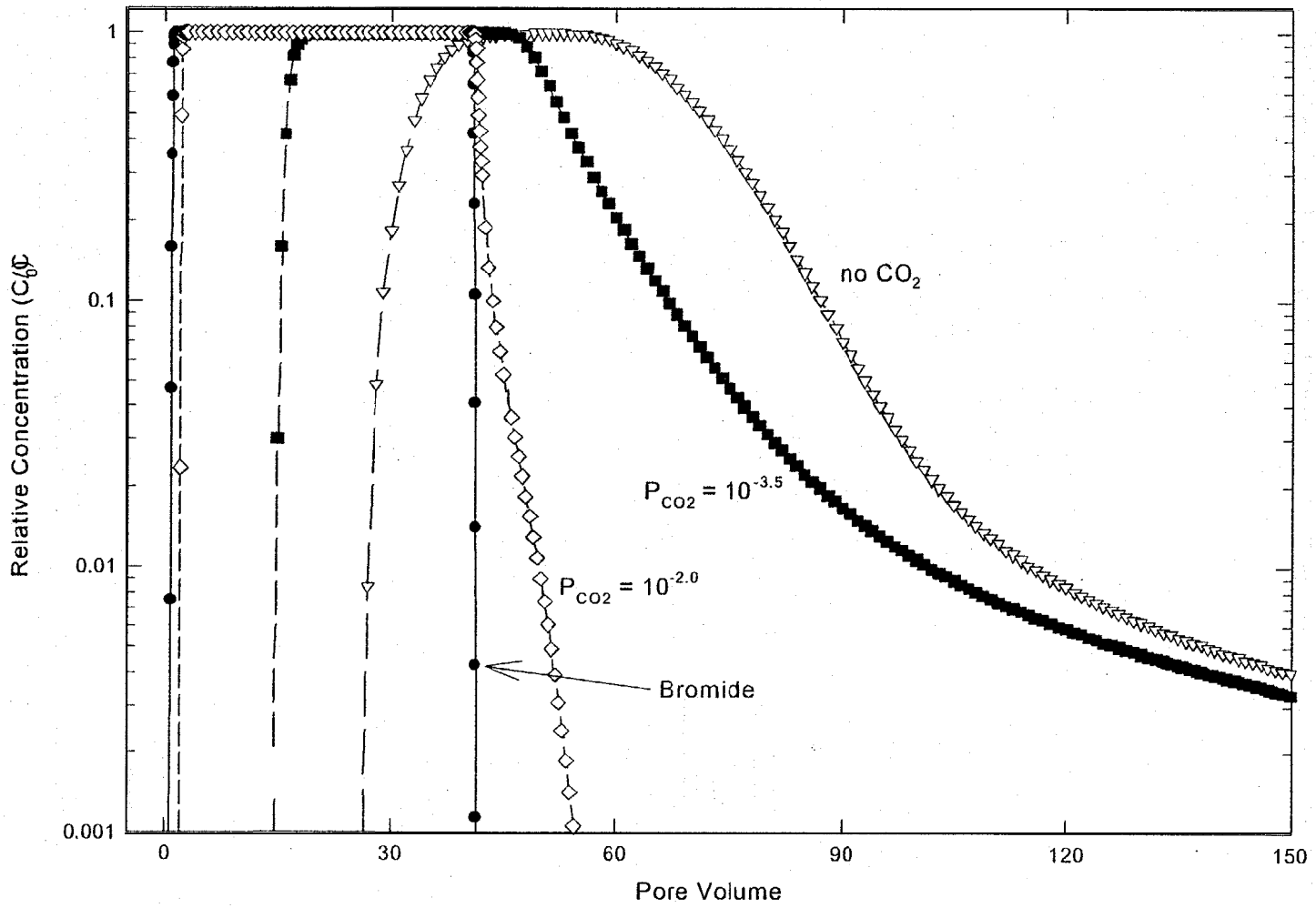

Fig. 3.7. Uranium breakthrough curves (relative concentration versus dimensionless time expressed as pore volumes) at different P_{CO2} values. Bromide is included as representative of a nonreactive tracer. Note that the y-axis is log scale to illustrate tailing behavior. $U_{TOT} = 10^{-5}$ M; pH = 7; I = 0.2.

4. REFERENCES

Bargar, JR, R Reitmeyer, JL Lenhart, JA Davis. 2000. Characterization of U(VI)-carbonato ternary complexes on hematite: EXAFS and electrophoretic mobility measurements. Geochim Cosmochim Acta. 64:2737-2749.

Barnett, MO, PM Jardine, SC Brooks, and HM Selim. 2000. Adsorption and transport of uranium(VI) in subsurface media. Soil Sci. Soc. Am. J. 64:908-917.

Grenthe, I, J Fuger, RJM Konings, RJ Lemire, AB Muller, CNT Cregu, and H Wanner. 1992. Chemical Thermodynamics of Uranium. North-Holland.

Jeter IW, and JM Napier. Chemical Analysis of the S-3 Disposal Ponds (April, 1978). Y/DA-7794. Union Carbide Corporation. 1978.

Lee, SY, LK Hyder, and PD Alley. 1987. Mineralogical characterization of selected shales in suuport of nuclear waste repository studies. Progress Report. ORNL/TM- 10567.

Luo, S, TL Ku, R Roback, M Murrell, TL McLing. 2000. In-situ radionuclide transport and preferential groundwater flows at INEEL (Idaho): Decay series disequilibrium studies. Geochim. Cosmochim. Acta. 64:867-881.

The Chemical and Radiological Characterization of the S-3 Ponds. Report Y/MA-6400. Union Carbide Corporation. 1983.

Waite, TD, JA Davis, TE Payne, GA Waychunas, and N Xu. 1994. Uranium(VI) adsorption to ferrihydrite: Application of a surface complexation model. Geochim Cosmochim Acta. 58:5465-5478.